Cave drip water solutes in south-eastern Australia: Constraining sources, sinks and processes

Carol V. Tadros [a,b,*], Pauline C. Treble [a,b], Andy Baker [b], Stuart Hankin [a], Regina Roach [c]

[a] ANSTO, Locked Bag 2001, Kirrawee DC, NSW 2232, Australia
[b] Connected Waters Initiative Research Centre, UNSW Sydney, Kensington, NSW 2052, Australia
[c] NSW National Parks and Wildlife Service, Sydney, NSW, Australia

HIGHLIGHTS

- Atmospheric inputs contribute to drip water: Na, K, Zn and other trace elements.
- K-fixation in soils controlled drip water K during the Millennium Drought.
- Na and K respond to soil processes and to higher water flux at drought termination.
- Zn colloidal mobilisation is linked to a decrease in soil pH.
- Na, K and Zn show promise as speleothem palaeo-climate proxies.

GRAPHICAL ABSTRACT

Sources, sinks and processes: Harrie Wood Cave, south-eastern Australia

ABSTRACT

Constraining sources and site-specific processes of trace elements in speleothem geochemical records is key to an informed interpretation. This paper examines a 10-year data set of drip water solutes from Harrie Wood Cave, south-eastern Australia, and identifies the processes that control their response to El Niño-Southern Oscillation events which varies the site water balance. The contributions of aerosol and bedrock end-members are quantified via hydrochemical mass balance modelling. The parent bedrock is the main source for the drip water solutes: Mg, Sr, K and trace elements (Ba, Al, V, Cr, Mn, Ni, Co, Cu, Pb and U), while atmospheric aerosol inputs also contribute significantly to drip water trace elements and Na, K and Zn. A laboratory investigation evaluating water-soluble fractions of metals in soil samples and soil enrichment factors provided a basis for understanding metal retainment and release to solution and transport from the soil zone. These results identified the role of the soil as a sink for: trace metals, Na and K, and a secondary source for Zn. Further, soil processes including: cation exchange, K-fixation, metal adsorption to colloids and the release of Zn associated with organic matter degradation further modify the chemical composition of the resultant drip waters. This research is significant for the south-eastern Australian region, as well as other sites in a karst setting with clay-rich soil. In particular these results reveal that the response of drip water chemistry to hydroclimatic forcing is non-linear, with the greatest response

* Corresponding author at: ANSTO, Locked Bag 2001, Kirrawee DC, NSW 2232, Australia.
 E-mail address: Carol.Tadros@ansto.gov.au (C.V. Tadros).

observed when the long-term gradient in the cumulative water balance reverses. This longer-term drip water monitoring dataset is significant because it provides the pivotal framework required to reliably identify suitable trace element proxies for interpretation in geochemical speleothem records on multi-decadal timescales.

1. Introduction

In eastern Australia, droughts, floods, bushfires, dust storms and cyclones are natural phenomena associated with El Niño and La Niña events with significant economic, social and environmental ramifications (Au, 2017). ENSO-related rainfall variability in south-east Australia has increased and these extreme weather events have become more frequent since 1950 (Nicholls, 2003). In Australia, ENSO is the main driver for dust events, where high dust activity is correlated with El Niño phases of the Southern Oscillation (Shao et al., 2013). Extended drought reduces vegetation cover and results in aeolian dust being transported from Australia's deserts, as well as from the alluvial and lacustrine environments of the Lake Eyre and Murray-Darling Basins, to Australia's east coast (Greene et al., 2009; Speer, 2013; Tadros et al., 2018). South-east Australia is also one of the most bushfire prone areas in the world. The current severity of bushfire events compared to observations since the 1940s, are related to more frequent hot and dry El Niño conditions (Lucas et al., 2007). Dust storms and bushfire events release significant amounts of aerosols to the atmosphere providing a novel opportunity to investigate in more detail, the potential contribution of dust to the trace element record in speleothems from south-east Australia (Rutlidge et al., 2014).

Aerosols are introduced into the atmosphere from sea spray, volcanic and geothermal activity and from biogenic emissions, as well as from anthropogenic sources such as mining, industry, agricultural and transportation sources (Tomasi et al., 2017). Dredge et al., 2013 presented the first investigation into the potential contribution of in-cave aerosols to speleothem geochemistry, highlighting the important role of aerosols as endmembers in the supply of trace elements (Tooth and Fairchild, 2003; Fairchild and Treble, 2009; Baldini et al., 2012; Tremaine and Froelich, 2013; Rutlidge et al., 2014; Treble et al., 2016). Based on atmospheric aerosol measurements over the years 2013–2017, Tadros et al. (2018) identified the chemical characteristics and sources of atmospheric aerosols in the Snowy Mountains alpine region, Yarrangobilly, SE Australia, postulating that deposited ambient particulate matter may be a significant source of trace metals to the site ecosystem. Trace elements are removed from the atmosphere by wet deposition (dissolved in precipitation) or by dry deposition of particles. Aerosols need to be considered as they may significantly affect the physical and chemical properties of karst soil (Rutlidge et al., 2014).

Above the cave, soil represents the major sink for trace metals released from the atmosphere and plays an important role in the retention and release processes (Kabata-Pendias, 2010). Generally, trace elements in the soil solution phase are affected by adsorption onto mineral surfaces or present as aqueous ions or solutes where they are mobilised through the soil profile. In solution they exist as: free trace metal ions (hydrated cations or oxyanions), as stable complexes with inorganic compounds or as organic compounds bound to suspended colloids including clay, organic matter and sesquioxides (Hartland et al., 2012). Trace elements in soil solution are biotransformed by microorganisms and also readily interact with biomass (Adriano, 2001; Hooda, 2010). Chemical weathering of bedrock through partial or complete dissolution, also releases rock-derived trace elements.

In karst environments, trace elements in soil solution may be leached and transported through the unsaturated zone, where further transformations occur. Between the soil zone and the cave ceiling, multiple hydrological flow pathways through the host rock and the capacity of storage, mixing and open system conditions can produce variations in the drip water trace element composition through dissolution-precipitation processes. Within the cave, increased ventilation and CO_2 degassing from drip waters or prior calcite precipitation (PCP), causes the removal of Ca through calcite precipitation along the flow path prior to reaching the stalagmite. Thus trace elements incorporated into speleothems have potential atmospheric, soil and bedrock sources. Dust transport, bushfires, weathering, and infiltration of meteoric water are often strongly influenced by climate. These events determine the supply of trace elements to the surface soil and bedrock, hence the drip-water thereby provides a potentially rich archive of palaeo-climate and palaeo-environmental information that is recorded in the geochemistry of stalagmites (Johnson et al., 2006; Siklosy et al., 2009; Sundqvist et al., 2013). Therefore, the motivation for the current research is to constrain sources and sinks and to differentiate between climate and karst processes impacting the drip water trace element composition in Harrie Wood Cave, Yarrangobilly, south-east Australia. This will build further validation on the potential use of trace elements as proxies for palaeo-environments.

In recent decades south-east Australia has experienced ENSO-related rainfall variability that has led to multi-year trends in the site water balance, including the Millennium drought from 1997 to 2009 that was followed by a short relatively wet phase during July 2010 to March 2011, and a dry episode in 2015 (BoM, 2017). A previous cave monitoring study from a different karst region in south-east Australia; Wombeyan Caves, located approximately 85 km from Harrie Wood Cave, demonstrated a relationship between PCP and climate (McDonald et al., 2004). McDonald et al. (2004) proposed that reduced recharge during the 2002–03 El Niño event resulted in more open system conditions, driving PCP and consequently raising drip water Mg/Ca and Sr/Ca ratios. At the current study site, Tadros et al. (2016) confirmed an enhanced PCP response to the 2006–07 and 2009–10 El Niño events. This longer study (2007–2013) also captured the opposite hydroclimate phase, the 2010–12 La Niña event that followed. Dilution dominated at the onset of the La Niña phase and a period of reduced PCP ensued in response to wetter conditions. Additional processes were also found to be linked to the extreme climate phases e.g. hydrological routing, and enhanced limestone dissolution mediated by microbial respiration in warmer soils was identified.

This research reports 10 years of cave drip water data (2007–2016) collected from three drip sites in Harrie Wood Cave, thus extending the dataset presented in Tadros et al. (2016) by a further three years. The objective is to firstly quantify the source(s) and sink(s) of solutes from Harrie Wood Cave. Secondly, to investigate the mobility of metals through the soil and assess processes which modulate the trace element concentrations in cave drip-water. This research is required for full characterisation of the source contributions and processes which have not yet been investigated for south-east Australia. Lastly, the implications of these findings for interpreting trace elements in stalagmite records for south-east Australia are also discussed.

2. Study area

2.1.1. Region and climate

The study site is located in the Snowy Mountains alpine region of south-eastern Australia along the Great Dividing Range. This region is the highest part of Australia and provides the headwaters to major river systems in the Murray Darling Basin, one of Australia's most important drainage basins (Fig. 1a). Situated in a temperate climate
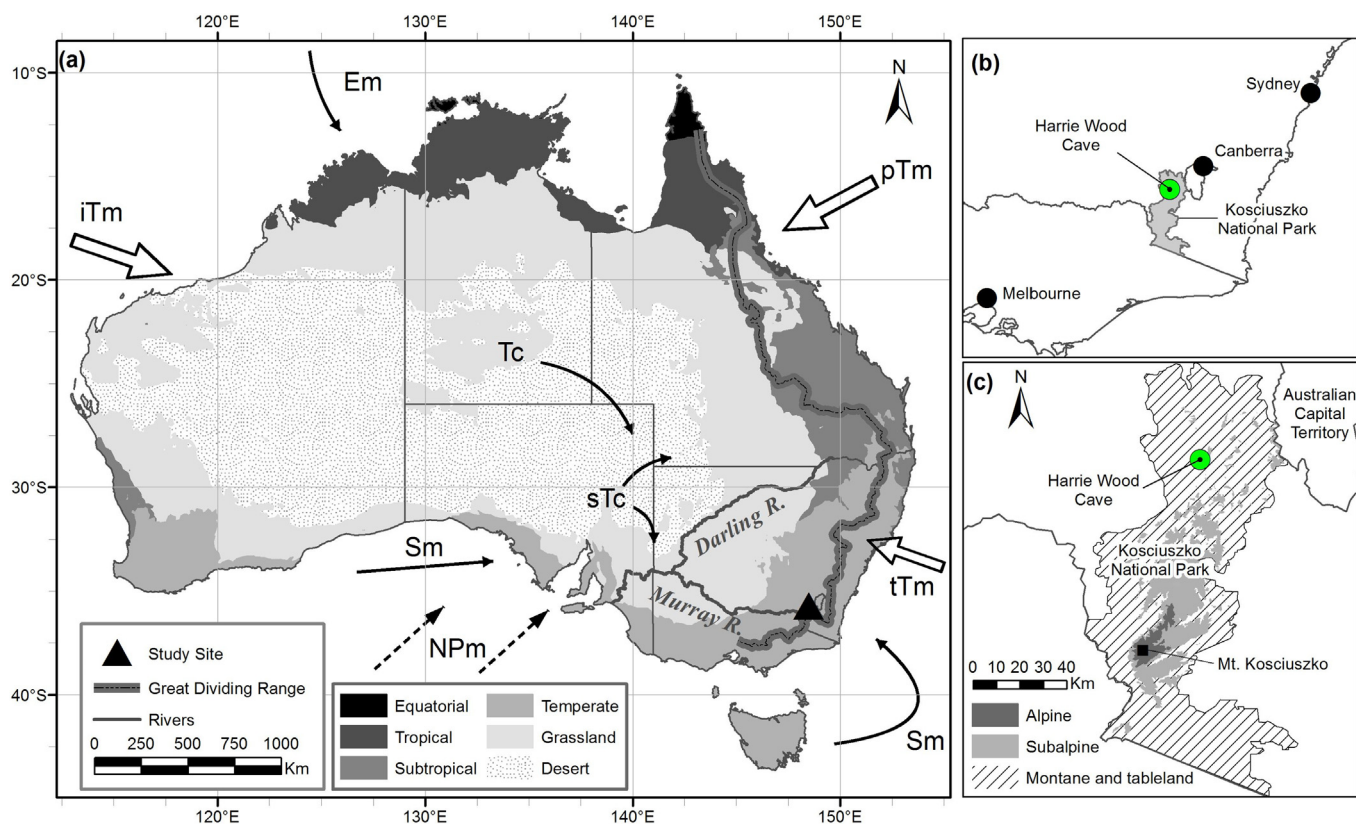
Fig. 1. (a) Map of Australia showing the study site location, Murray-Darling river system and Great Dividing Range. Also shown are the major climate zones (BoM) and eight major air-mass types affecting weather across Australia: modified polar maritime (NPm); Southern maritime (Sm); Tropical maritime Tasman (tTm); Tropical maritime Pacific (pTm); Tropical maritime Indian (iTm); Equatorial maritime (Em); Tropical continental (Tc); and Subtropical continental (sTc) (after Sturman and Tapper, 1996). (b) Location of the study site within Kosciuszko National Park (Shaded). (c) Physiographic bioregions in the Australian Alps in south-eastern Australia (elevation data: Creative Commons 4.0 International License; classification after Pickering and Growcock, 2009).

zone, the region receives a median rainfall amount of 1178 ± 29 mm annually (Tadros et al., 2016); however significant interannual rainfall variability in the region is recognised as being influenced by ENSO (Dai et al., 1997; Risbey et al., 2009). The mean wintertime (austral June–August) maximum rainfall was 349 ± 15 mm over the period 1985–2015, based on records from the closest Bureau of Meteorology (BoM) weather station at Yarrangobilly Caves (BoM station 72141). Increased rainfall in the study region during winter (JJA) is due to cut-off lows, cold fronts and pre-frontal airflow strongly influenced by the mid-latitude westerly wind belt (Chubb et al., 2011; Pook et al., 2014; Callow et al., 2014; Theobald et al., 2016). During winter, the Southern maritime (Sm) and polar maritime (Npm) air masses bring cool, moist and unstable air arising in the Southern Ocean to south-eastern Australia (Fig. 1a; Sturman and Tapper, 1996). During the warmer months in the austral summer (DJF), inland heat troughs and lows from the tropical latitudes results in lower precipitation overall (Theobald et al., 2016), with a summertime minimum rainfall amount of 191 ± 5 mm (BoM station 72141). These tropical continental (Tc) air masses which arise over Central Australia are very hot, and dry, and may bring heatwave conditions to southern Australia in summer under a strong northerly air flow. Also, southern maritime (Sm) air masses, as a result of high pressure systems, bring easterly winds to the east coast of Australia during summer (Sturman and Tapper, 1996).

Situated on the western slopes of the Great Dividing Range, the study site is exposed to winds that have passed over Australia's deserts, receiving 11.3 ± 0.5% of fine particulate matter in air from soil containing aeolian salts originating from the inland salt source regions of the Lake Eyre and Murray Darling Basins and agricultural regions in the Murray Darling Basin (Johnston, 2001; Tadros et al., 2018). Our inland high altitude study site is approximately 152 km from the Pacific Ocean on the south-east coast of Australia and wind-blown salt from

aged sea spray from the Southern Ocean contributes 10.1 ± 0.4% to the total airborne particulate matter (Tadros et al., 2018).

The study site is located in Kosciuszko National Park (Fig. 1b) and with an area of 6900 km² the Park is covered by four physiographic bioregions, including alpine, sub-alpine, montane and tableland (Fig. 1c). Our study site lies within the montane area of the bioregion and surrounding vegetation currently consists of open snowgum (*Eucalyptus pauciflora* subsp. *Pauciflora*) and black sallee (*E. stelullata*) woodland with a snow grass (*Poa sieberi*) dominated understorey (Aplin et al., 2010). Bushfires and hazard reduction burns are a common occurrence of the park ecosystem that produce transient peak smoke emissions of airborne particulate matter (Wotawa and Trainer, 2000; Tadros et al., 2018). Furthermore, drought and El Niño conditions increase terrestrial soil-derived and smoke aerosol loadings at Yarrangobilly (Tadros et al., 2018). Coleborn et al., 2018 demonstrated, soluble ash-derived metals from fires occurring directly above a cave site can be mobilised; influencing the drip water geochemistry for up to one year after a fire. In January 2003, the Australian Alps, including the surface environment directly above Harrie Wood Cave, were affected by the largest bushfires in more than 60 years (Tadros et al., 2016). This occurred four years prior to the commencement of the long-term cave drip water monitoring study at Harrie Wood Cave and as such the impact of the intense bushfire on data presented here is negligible.

2.1.2. Location

The study site is located at Yarrangobilly Caves; formed within a Late Silurian limestone block, of approximately 18 km², and containing extensive independent cave systems. This research uses drip-water data collected over 10 years from three monitoring drip sites (HW1, HW2 and HW3). The drip sites are active stalactites, centrally located in Harrie Wood Cave (35° 44′S, 148° 30′E; 965 m a.s.l; Fig. 1b). A survey

map of the drip sites and a detailed description of the drip collection setting were previously published in Tadros et al. (2016).

Soils above Harrie Wood Cave lack horizons, are rocky and relatively shallow (~0–0.5 m deep) on highly fractured hard massive limestone (~34 m thick). The different flow routes within Harrie Wood Cave have been characterised by extensive drip water logging (Markowska et al., 2015). Importantly, the hydrochemical investigation of the drip waters by Tadros et al. (2016) confirmed the flow path of karst waters through the aquifer to drip sites HW1-3 are fed by fracture flow from a well-mixed pocket reservoir with variable head space, within the epikarst storage reservoir.

3. Methods

3.1. Rainfall, soil moisture and cumulative water balance

Daily rainfall totals (reported to 0.1 mm) were obtained from the Bureau of Meteorology (BoM) rainfall gauge at Yarrangobilly Caves (BoM station 72141). Data from 2007 to 2013 were presented in Tadros et al. (2016) and were updated to July 2016 for this investigation.

Soil moisture saturation, at a depth of 25–30 cm, is measured at two sites above Harrie Wood Cave by a Stevens Hydra Probe®. Soil moisture is sampled at 15-min intervals and the water fraction volume (accuracy; 3% v/v) is recorded by a dataTaker DT80 data logger (Tadros et al., 2016). Soil moisture data from October 2011 to December 2012 and December 2012 to April 2016 were presented in Markowska et al. (2015) and Coleborn et al. (2018), respectively. These two dataset were combined and updated in this paper to August 2016 to form a continuous time series from October 2011 to December 2016. Markowska et al. (2015) showed that when the water fraction of the total soil volume (L_{water}/L_{soil}) lies between a field capacity of 0.30 and 0.45 (L_{water}/L_{soil}), rainfall events >13 mm infiltrated initiating an increased discharge response. As such, infiltration is inferred from the soil moisture data when rainfall events exceed a recharge threshold of 0.30 (L_{water}/L_{soil}) or in the absence of soil moisture data, when rainfall events exceed 13 mm.

The cumulative water balance (CWB) represents the monthly water budget trend at the study site and is calculated as the cumulative sum of the monthly precipitation minus evapotranspiration. CWB data from 2007 to 2013 were presented in Tadros et al. (2016) and updated to 2016 for this investigation to distinguish between wet and dry rainfall periods.

3.2. Drip water analyses

Cave drip waters were collected at a two-week frequency from three drip sites (HW1, HW2 and HW3) over the period July 2006 to July 2016 (n = 642). At each drip site, two 50 mL aliquots from the bulk drip water sample, collected in 1 L HDPE containers, were filtered through a mixed cellulose ester 0.45 μm filter into polypropylene bottles and refrigerated until analysis. A description of the parameters measured, collection methodology and apparatus are specified in Tadros et al. (2016). Drip water Ca, Cl, Mg/Ca and Sr/Ca datasets, between July 2006 and December 2013, from the three drip-water monitoring sites (HW1–3), were previously reported in Tadros et al. (2016) and updated to July 2016. In addition the solutes: Na, SO₄, K, Ba, Al, As, V, Cr, Mn, Ni, Co, Cu, Zn, Pb and U have not been previously investigated and are examined in this paper.

Prior to cation analysis, one 50 mL drip water sub-sample was acidified with 0.5 mL Merck Suprapur® 65% HNO₃. For the drip water samples, Ca, Mg, Sr, K, and Na were measured on a Thermo Fisher iCAP7600 inductively coupled plasma-atomic emission spectroscopy (ICP-AES) at ANSTO, while Ba, Al, As, V, Cr, Mn, Ni, Co, Cu, Zn, Pb and U were below the limit of detection. Therefore ultra-trace concentrations of these elements from drip site HW1 were measured on a Varian 820MS inductively coupled plasma-mass spectrometry (ICP-MS) at ANSTO. Rh and

In were used as an internal standards for ICP-AES and Li, Sc, Rh, In, Re and Bi for ICP-MS to correct for instrument drift, matrix effects and plasma fluctuations. A set of standards from 0.005–50 ppm for ICP-AES and 1–500 ppb for ICP-MS were also analysed after every 20th sample to monitor for instrument drift. An in-house reference sample was analysed in each ICP-AES run to check reproducibility between runs. The in-house reference sample was made to have concentrations of 55 ppm Ca, 1.2 ppm Na, 0.53 ppm Mg, 0.1 ppm K, 0.048 ppm Sr and 0.006 ppm Ba, similar to the cave drip water levels. All standards were prepared from certified single element standards (1000 ± 3 ppm) and National Institute of Standards and Technology (NIST) traceable. Anion concentrations; Cl and SO₄, on the un-acidified 50 mL drip water sub-samples were determined by ion chromatography (IC) using a Dionex DX-600 ion chromatograph with a self-regenerating suppressor at ANSTO.

3.3. Soil and bedrock analyses

Five surface soil samples were collected on the slope above Harrie Wood Cave with a 48 mm diameter × 45 mm height stainless steel corer. Soil samples were stored in polyethylene bags and refrigerated at 4 °C until analysis. The sampling protocol for the bedrock samples used in this investigation (n = 4; YGB_R7 – R10) are described in Tadros et al. (2016). Only the Ca concentrations and Mg/Ca and Sr/Ca ratios of the bedrocks were previously investigated in detail (Tadros et al., 2016).

Bulk bedrock and soil samples were oven-dried (40 °C) and powdered. A subset of each sample (0.2 g) was then microwave digested (180 °C for 15 min) in aqua regia (1 mL HCl: 3 mL HNO₃) and diluted to 30 ml for the elemental analysis of the non-silicate component by ICP-AES at ANSTO.

Leaching experiments to simulate infiltration from rainfall and assess the mobile, water soluble fractions of metals in soil samples, were conducted in triplicate using the extraction procedure of Tessier et al. (1979) as described in Ma and Rao (1997). The soil samples were sieved to pass a 2.36 mm stainless steel screen and the <2.36 mm fraction was used. The samples were oven-dried at 40 °C to constant weight. One gram of each soil sample was weighed into a 50 mL polypropylene centrifuge tube. The water soluble fraction was extracted with 30 mL of deionised water for 2 h. The supernatants were filtered through 0.2 μm polyethersulfone filters and preserved by acidification with Merck Suprapur® HNO₃ for metal analysis. The concentration of: Na, Mg, Al, P, S, K, Ca, Sc, Fe and Y were determined by ICP-AES while other trace metal concentrations were determined by ICP-MS at ANSTO. Soil pH measurements were performed on a 1 part soil to 5 part water suspension (Rayment and Higginson, 1992).

3.4. Data processing

3.4.1. Mass balance model

The mass balance equation is used to calculate for each element, the net concentration (mg L^{-1}) added by a source or removed from solution by a sink. A mass balance should be conducted over a sufficiently long time scale otherwise variability in the system may contribute to large uncertainties (Drever, 1997). Therefore, we adopted the mass balance model outlined by Treble et al. (2016), and summarised in Table 1, to quantify sources and sinks of elements within the karst system using the full 10-year data set. Data collected from the measurement sites, provides well-defined end-member sources. First, the mass balance is performed to quantify the drip water solute concentration from marine aerosol and bedrock contributions by solving Eqs. (1) and (3) (Table 1), respectively. As in Treble et al. (2016), the minimum measured drip water ratio prior to any impact of PCP, [Mg/Ca]$_{PCP}$, was applied to estimate the initial Ca concentration, [Ca]$_{initial}$. The PCP correction was then applied for Mg and Sr (Eq. (4); Table 1) and accounted for 0.7 to

Table 1

Summary of the overall mass balance equation and equations used to calculate the concentration of marine aerosol, nss aerosol, bedrock and residual contribution to the cave drip water samples.

Contribution	Equation (s)		Remarks
Marine aerosol	$[ion]_{marine\ aerosol} = [Cl]_{dw} \times [ion/Cl]_{seawater}$	[1]	[ion/Cl] molar ratios of major ions in seawater (Na, Mg, SO$_4$, Ca, K and Sr) were taken from Chester (2009).
Non-sea salt aerosol	$[ion]_{nss} = [S]_{dw} \times [(ion/S)_{atm}]_{nss}$ where: $[ion_{atm}]_{nss} = [ion_{atm}] - ([Cl_{atm}] \times [ion/Cl]_{seawater})$	[2]	S is used as a tracer of atmospheric aerosols (Sarnat et al., 2002). [ion/Cl] molar ratios of trace ions in seawater were taken from Turekian (1968)
Bedrock	$[ion]_{bedrock} = [Ca]_{initial} \times [ion/Ca]_{bedrock}$ where: $[Ca]_{initial} = [Mg]_{dw} / [Mg/Ca]_{PCP}$	[3]	For each drip site, [Mg/Ca]$_{PCP}$ corresponds to the minimum measured drip water ratio prior to PCP.
PCP	$[ion]_{PCP} = [Ca]_{PCP} \times [ion/Ca]_{dw} \times K_{Mg}$ where: $[Ca]_{PCP} = [Ca]_{initial} - [Ca]_{dw}$	[4]	[ion]$_{PCP}$ calculated for Mg and Sr only Partition coefficients: $K_{Mg} = 0.019$ (Huang and Fairchild, 2001) $K_{Sr} = 0.1$ (Fairchild and Baker, 2012).
Residual	$[ion]_{residual} = [ion]_{dw} - [ion]_{marine\ aerosol} - [ion]_{nss} - [ion]_{bedrock} + [ion]_{PCP}$	[5]	A positive residual value indicates an additional source not constrained by the end-members, while a negative residual value indicates a sink.
Overall	$[ion]_{drip\ water} = [ion]_{marine\ aerosol} + [ion]_{nss} + [ion]_{bedrock} + [ion]_{residual}$	[6]	

1.1% of Mg concentrations in drip water and 3.8 to 6.0% of Sr concentrations in drip water.

Next, since Harrie Wood Cave receives atmospheric aerosols from local and long-range transport (Section 2.1.1), we also take into account the contribution of non-sea salt (nss) pollution and dust which was not relevant at the study site of Treble et al. (2016). We therefore perform an additional calculation to Treble et al. (2016) to estimate this from our previously published aerosol measurements (Tadros et al., 2018). Hence, the nss aerosol contribution was calculated by solving Eq. (2) (Table 1).

Lastly, as in Treble et al. (2016), sinks, additional sources and processes that cannot be constrained are accounted for in the mass balance model via a residual term and are calculated using Eq. (5) (Table 1). A positive residual value indicates an additional source not constrained by the end-members, while a negative residual value indicates a sink. The overall mass balance equation used is summarised by Eq. (6) (Table 1).

3.4.2. Enrichment factors

Enrichment or depletion of trace elements in the soil was assessed by calculating the enrichment factors (EF) of elements in the bulk soil relative to the bulk bedrock material. This calculation is based on the concentration of an element X in the soil to the bedrock, and referenced to a chemically inert element:

$$EF = [X/Zr]_{soil} / [X/Zr]_{bedrock} \qquad (7)$$

where X is the element, a square bracket denotes concentration (mg kg^{-1}) and Zr represents Zirconium, the reference element. We use chemical bedrock data obtained from our site as a more accurate representation of the bedrock starting composition, rather than the average crustal rock concentration (Bowen, 1979; Taylor and McLennan, 1995).

4. Results

4.1. Mass balance

The contribution of marine aerosol, nss aerosol, bedrock and residuals to the drip water geochemistry are quantified in Table 2, and are similar across the three drip sites. Drip water Mg concentrations are mainly sourced from the bedrock (97–99%), with 16% supplied from marine aerosols and the residual term indicating a 13–16% sink. Sr is derived from the local bedrock with 2% or less from other sources and a negligible residual term. Bedrock is also the dominant source of K concentration in drip waters (138–146%) with significant additional

contributions supplied from marine aerosols (23–25%) and nss atmospheric input (20–22%). The large negative residual term indicates a significant sink for K. Drip water Na concentrations are predominantly from marine (95–100%) and also atmospheric nss supplied aerosols (28–29%). A sink for Na is also indicated by the negative residual term. The cave drip water receives 37–38% of their S input from marine aerosols and 4% from the bedrock. This suggests that qualitatively the nss contribution will be at least 60%, but this cannot be quantified due to method assumptions.

For the trace metals: Al, V, Cr, Mn, Ni, Co, Cu, Zn, Pb and U mass balance data shows that the contribution from marine aerosols is negligible (<0.1%) while atmospheric deposition of nss aerosols supplies a substantive contribution to the resultant cave drip water solution (Table 2). However the bedrock-derived contributions for these trace metals, except for Zn, are significantly over-estimated. This may be attributed to analysis by different techniques: ICP-AES and ICP-MS (Section 3.2) however drip water Sr concentrations duplicate well using the two techniques. Alternatively, this could be a consequence that the analytical conditions i.e. acid digestion of bedrock, resulting in higher trace metal concentrations than those derived under field conditions. Nevertheless, the mass balance data indicates the bedrock is by far the main source of these dissolved constituents in the drip water. The contribution of Zn from the bedrock is lower (27%) and this could be considered to be a maximum given that the bedrock contributions are over-estimated. While the concentration of the Zn in the drip water is comparable to the other trace metals, the results of the acid leaching do show that Zn in the bedrock is three orders of magnitude lower than the other trace metals (Table. A.1). Overall, these calculations estimate that the quantifiable Zn end-members contribute 44% to drip water and that there is an additional source of Zn to be considered, indicated by the large positive residual (55%). We interpret this result to suggest that the soil is a secondary source. Other drip water trace metals, as well as Na and K, have significant negative residuals. This indicates a sink and it is likely that large quantities of these mostly derived bedrock metals are retained in the soil, consistent with a soil sink. The role of the soil in these processes is considered below.

4.2. Enrichment factors and metals in soil water extracts

Table 3 lists laboratory measured soil pH together with the water extractable metal concentrations of the soil samples. The solubility of metals, thus their concentration in the soil water extracts is a direct indication of mobilisation from the soil zone to the aqueous phase. A compilation of the geochemical data for 24 elements in bulk soil (n = 4) and bedrock samples (n = 4) is included in Table A.1.

Table 2
Average drip water concentrations (n = 642) and contribution of individual elements sourced from end-members (see Table 1 for details) for each drip site HW1, HW2 and HW3. Dividing the averaged values by the average drip water concentration enabled the percentage contribution of the ions to be calculated. The drip water S concentration is calculated from SO_4. #; the residual component for Mg and Ba is calculated without the nss atmospheric component, as this could not be analytically determined in the aerosol study (Tadros et al., 2018). * indicate elements re-analysed by ICP-MS for drip site HW1 only. n.d., not determined as S is used as a nss atmospheric tracer. n.a., not applicable.

ICP-AES

Ion	Drip water concentration (mg l⁻¹)			Marine aerosol contribution (%)			Atmospheric nss contribution (%)			Bedrock contribution (%)			Residual contribution (%)		
	HW1	HW2	HW3	HW1	HW2	HW3	HW1	HW2	HW3	HW1	HW2	HW3	HW1	HW2	HW3
#Mg	0.58	0.58	0.58	17	16	16	n.a.	n.a.	n.a.	99	98	97	-16	-13	-13
Sr	0.05	0.05	0.05	1	1	1	2	2	2	101	102	100	0	1	1
Na	0.81	0.82	0.83	100	96	95	29	28	28	1	1	1	-31	-26	-25
K	0.12	0.13	0.12	25	23	24	22	20	21	146	138	141	-93	-81	-86
S	0.18	0.18	0.18	38	37	37	n.d.	n.d.	n.d.	4	4	4	n.d.	n.d.	n.d.

ICP-MS

Ion	Drip water concentration HW1 (mg l⁻¹)	Marine aerosol contribution HW1 (mg l⁻¹)	%	Atmospheric nss contribution HW1 (mg l⁻¹)	%	Bedrock contribution HW1 (mg l⁻¹)	%	Residual contribution HW1 (mg l⁻¹)	%
#Ba	0.01	1.6E-06	< 0.1	n.a.	n.a.	4.5	>>100	-4.53	n.a.
*Al	3.4E-02	7.5E-08	< 0.1	1.7E-02	50	0.42	>>100	-0.40	n.a.
*V	1.1E-04	1.4E-07	< 0.1	2.1E-04	185	6.8E-04	>>100	-7.8E-04	n.a.
*Cr	1.4E-03	1.5E-08	< 0.1	4.0E-04	28	0.4	>>100	-0.37	n.a.
*Mn	1.1E-03	3.0E-08	< 0.1	5.4E-04	48	0.01	>>100	-0.01	n.a.
*Ni	3.3E-03	5.0E-07	< 0.1	4.4E-04	14	1.8	>>100	-1.79	n.a.
*Co	4.4E-04	2.9E-08	< 0.1	2.6E-04	61	1.3	>>100	-1.34	n.a.
*Cu	5.8E-03	6.8E-08	< 0.1	7.5E-04	13	0.3	>>100	-0.26	n.a.
*Zn	4.5E-03	3.8E-07	< 0.1	7.9E-04	17	1.2E-03	27	2.5E-03	+ 55
*Pb	6.2E-03	2.3E-09	< 0.1	7.7E-04	12	0.58	>>100	-0.58	n.a.
*U	6.7E-05	2.5E-07	< 0.1	n.a.	n.a.	0.06	>>100	-0.06	n.a.

Under experimental conditions, the detected solutes leached from the soils were, in order of highest to lowest concentration, in mg kg⁻¹: Ca, K, S, Na, Mg, Al, and in µg kg⁻¹: Sr, Mn and Ba (Table 3). Hence we infer that these metals are mobilised from the soil during rainfall. While the metals: V, Cr, Co, Ni, Cu, Zn and Pb were detected in bulk soil digestions (Table A.1), they were not detectable in the water extracts, likely indicating formation of metal complexes with insoluble soil organic matter.

Fig. 2 shows the relative enrichment and depletion of metals in soils, compared to the composition of the bedrock. The soil enrichment factors indicate that the trace metals: Al, S, K, V, Cr, Mn, Ni, Cu, Zn, Ba and Pb, are retained in the soil (EF ± s.d. > 1; Fig. 2) and the EF for Na is approximately 1, thus confirming the soil is a significant net sink for these metals. Conversely, enrichment factors for Mg, Ca and Sr are <1 consistent with their high abundance in the bedrock.

Zinc concentrations measured in the soil were 40 times higher than the bedrock in the bulk digestion experiments (Table A.1). Zn is retained in the soil (Fig. 2) and from the leaching experiments is inferred to be complexed with organic matter (Table 3). Soil pH was in the range 6.98 to 7.37 (Table 3). Hence it is plausible that under field conditions,

Zn may be released in soil solution becoming a secondary source, if soil pH is lower than the range recorded in Table 3.

Bulk digestion data show that K is retained in the soil (Fig. 2) and is readily released under the leachate experimental conditions (Table 3). In contrast, other chemically similar solutes i.e. Na that are also readily released in the leachates are not as strongly retained in the soil (Fig. 2). This difference is attributed to the fact that K-fixation is non-exchangeable compared to the cation exchange reactions that is acting on Na, which we further consider below.

4.3. Drip-water chemistry

Time series of Cl, Na, Na/Cl, SO_4, Ca, Mg, Sr and K concentrations in drip site HW1–3 and Zn concentrations in drip site HW1 are presented in Fig. 3, together with the daily rainfall, infiltration, cumulative water balance (CWB) and soil moisture. No clear trends were observed in the drip water dataset for any of the detectable minor elements: Al, As, Ba, Co, Ni and U (Fig. A.1). Principal component analysis (PCA) was carried out for seven variables (Ca, Cl, Mg, Na, SO_4, K and Sr) in each drip water dataset from 2009 to 2016 in order to identify processes

Table 3
Summary of soil pH and metal concentrations, mean ± standard deviation (s.d.), in the soil water extracts. Concentrations of: V, Cr, Co, Ni, Cu, Zn and Pb were below the detection limit of 20 µg kg⁻¹.

Sample code	pH	Na (mg kg⁻¹)	Mg (mg kg⁻¹)	Al (mg kg⁻¹)	S (mg kg⁻¹)	K (mg kg⁻¹)	Ca (mg kg⁻¹)	Mn (µg kg⁻¹)	Sr (µg kg⁻¹)	Ba (µg kg⁻¹)
YGB_S1	7.34 ± 0.09	5.9 ± 0.2	4.8 ± 0.3	1.9 ± 0.3	6.9 ± 0.3	12.2 ± 0.5	225 ± 12	43 ± 4	143 ± 5	20 ± 2
YGB_S2	6.98 ± 0.04	7.5 ± 0.1	4.8 ± 0.1	2.1 ± 0.1	6.2 ± 0.1	8.3 ± 0.2	201 ± 5	55 ± 9	136 ± 18	20 ± 6
YGB_S3	7.00 ± 0.06	4.6 ± 0.1	5.1 ± 0.1	1.4 ± 0.2	6.7 ± 0.1	15.9 ± 0.5	222 ± 5	59 ± 10	153 ± 8	19 ± 2
YGB_S4	7.07 ± 0.08	6.7 ± 0.1	3.5 ± 0.02	1.5 ± 0.1	6.7 ± 0.3	9.3 ± 0.2	210 ± 4	50 ± 2	142 ± 14	21 ± 0
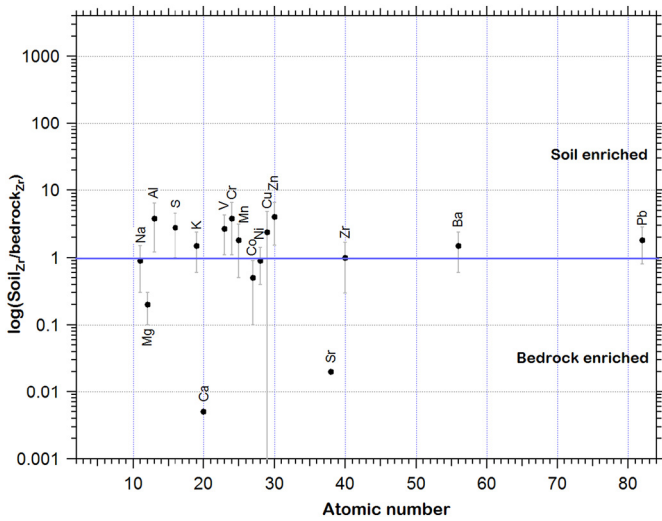
Fig. 2. Soil EF relative to the bedrock material as a function of atomic number, the error bars are one s.d. Values > 1 denote the enrichment of the element in the soil relative to the bedrock and values < 1 indicate depletion in the soil profile relative to the bedrock. For soil and bedrock chemical data see Table A.1 in Supplementary.

driving the trends in the drip water chemistry. The first three principal components (PC1, PC2 and PC3) accounted for 87.1%, explaining most of the variance in the drip water dataset (Table A. 2), though the temporal variation in each PC closely corresponded to the time series of the highest factor loading for each variable (Fig. A.2). PCA highlighted that the original data can be used to gain a better understanding of the processes dominating changes in the drip water.

November 2006 to June 2010 was the driest period, apparent by the sharp decline in the cumulative water balance (Fig. 3a), and coincided with the latter four years of the Millennium drought. Overall, Cl, Na

and SO_4 concentrations were higher during this period (Fig. 3c, d and f), but were also declining during this drying period. Drip water Na/Cl ratios are greater than the seawater ratio of 0.86 (Fig. 3e) and the regression slope of Na vs. Cl during these drier years is 1.02 (Fig. A.3), this is consistent with the mass balance results (Section 4.1; Table 2) confirming the contribution of Na from non-sea salt sources. Tadros et al., 2016 suggested that the decreasing Cl trend during this interval was due to a decreasing supply from a salt rich soil source over time. The initially enhanced Na/Cl ratio from this research confirms this. Solutes Ca, Mg and Sr largely show similar trends during the dry period, with the exception of the shift to higher Mg and Sr in late 2007 owing to a flow path change (Tadros et al., 2016). The rise in Ca concentrations from ca. 60 mg L^{-1} in 2008 to ca. 80 mg L^{-1} in November 2009 was attributed to enhanced weathering due to increased CO_2 in the soil atmosphere from soil microbial activity (Tadros et al., 2016).

The cumulative water balance increased overall between July 2010 and April 2012 (Fig. 3a) and soil moisture data collected from probes installed in October 2011 demonstrate that soil moisture was above the field capacity threshold during this period (Fig. 3b). This period was the 2010–12 La Niña event, one of the strongest on record which resulted in above average rainfall at Yarrangobilly Caves (BoM, 2017; Tadros et al., 2016). Sodium concentrations sharply decline at the onset of this period of higher water flux (Fig. 3d). Fig. 3e shows that the Na/Cl ratios fall to approximately the seawater ratio (HW1 and 3) or below (HW2) coinciding with infiltration. Throughout the following wetter period, drip-waters show a variable and wide range of Na/Cl ratios (0.6–1.1) but overall, the regression slope that represents the Na vs. Cl ratios (0.66) during this wetter period is <0.86 (Fig. A.3). Conversely, the concentration of the divalent cations, Ca, Mg and Sr initially increase (Fig. 3g, h and i); then show greater short-term variability relative to the preceding dry period. When infiltration first increases after a dry period, it may be reasonable to attribute higher drip water Ca, Mg, and Sr concentrations to increased mineral weathering, however we argue that the enrichment of Ca, Mg and Sr, accompanied by a depletion
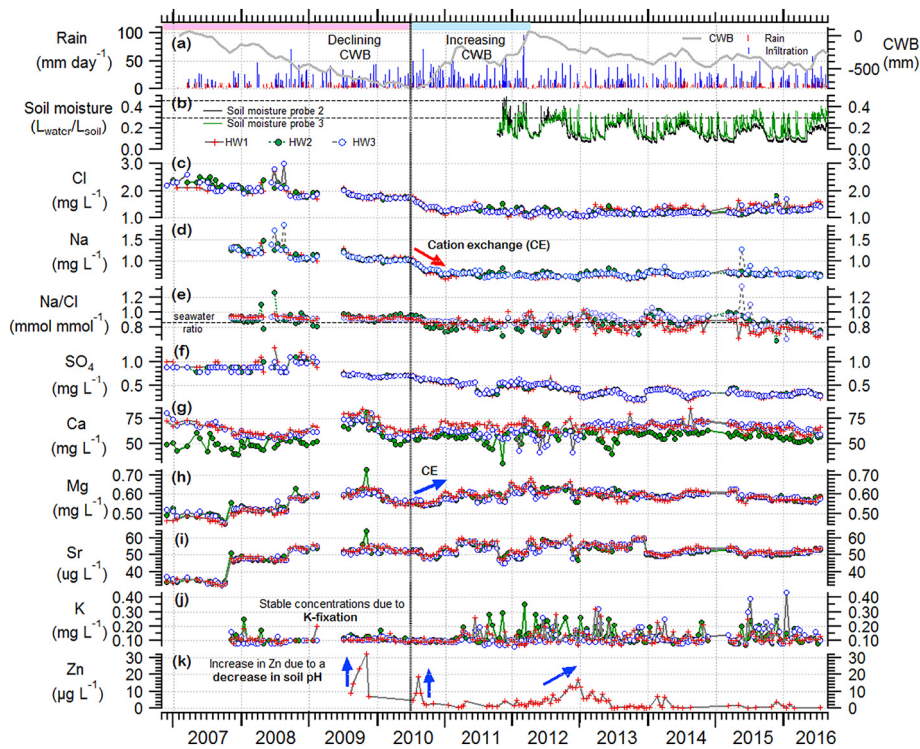
Fig. 3. Time series of (a) daily rainfall, inferred infiltration (Section 3.1) and cumulative water balance (CWB) and (b) soil moisture; the recharge threshold range between 0.30 and 0.45 (L_{water}/L_{soil}) is indicated by the horizontal dotted lines. Drip water (c) Cl, (d) Na, (e) Na/Cl, (f) SO_4 (g) Ca, (h) Mg, (i) Sr and (j) K concentration at drip sites HW1 – HW3 and (k) Zn concentration at drip site HW1. The pink and blue coloured bars at the top correspond to a decline and increase in the CWB, respectively and the black vertical line at July 2010 signifies the onset of the wet 2010–12 La Niña event. (For interpretation of the references to colour in this figure legend, the reader is referred to the web version of this article.)

of Na, indicated by Na/Cl less than seawater, provides evidence that cation exchange processes also occurred. It is proposed that the mobilising of Na-rich water from the soil during the initial recharge event, results in the uptake of Na by the soil exchanger. This is expressed as a drop in drip water Na and Na/Cl ratios, with the concomitant release of Ca, Mg and Sr, and respective increase in drip water concentrations. Unlike the elements involved in clay cation exchange, SO_4 behaves differently showing a long-term decrease in concentrations by 60% from July 2010 to July 2016. This suggests the declining drip water SO_4 may be driven by an alternate process, for example uptake into biomass (Treble et al., 2016).

K has a fairly stable concentration during the Millennium drought, the enhanced weathering episode in 2009 and is sustained during the onset of the wetter period in July 2010 (Fig. 3j). This stability indicates the uptake of water-soluble K into internal clay surfaces and becomes non-exchangeable in the soil. However, a clear transition is observed in March 2011 once water balance has been restored to relatively wetter conditions. At this time, K concentrations increase and become more variable, evident by transient peaks of 1–2 months, indicating K is released into solution as the clay particles are weathered. This pattern appears only for K; strongly supporting the interpretation of K-fixation by clay minerals.

During the Millennium drought, Zn concentrations peaked at the same time as Ca in late 2009. The rise in Ca was interpreted to be due to an increase in carbonic acid under elevated soil CO_2 from microbial respiration (Tadros et al., 2016). Disassociation of carbonic acid causes an increase in HCO_3^- which is also accompanied by an increase in H^+ or decrease in pH, in turn supporting our hypothesis of Zn colloidal mobilisation from soils when pH is lowered. There are two further periods of higher Zn concentrations: a pulse in August 2010 and a gradual increase in 2012. The cause of the short-lived pulse in 2010 is ambiguous, however during the longer rising trend in 2012, Zn appears to become mobilised when the cumulative water balance reverses to a declining trend.

From April 2012 soil moisture capacity was less frequently above field capacity however the cumulative water balance slowly declined through to the end of the study in July 2016, but was still higher compared to the earlier Millennium drought period. Although soil moisture data was not available for the Millennium drought period for comparison, from this trend we infer reduced inflow from the soil storage to epikarst storage reservoir. The impact of the 2015–16 El Niño, between April 2015 to April 2016, on the site cumulative water balance was marginal and this was also reflected in the drip water chemistry (Fig. 3). This is interpreted to indicate that variability in cave drip water chemistry increases when there is an increase to the site's cumulative water balance. In this investigation, this was instigated by the transition between the Millennium Drought and 2010–12 La Niña event.

5. Discussion

5.1. Source of drip water ions from end-members

Based on the mass balance calculations, the limestone bedrock is the primary source of Mg, Sr and K, as well as trace elements, to the drip water (Section 4.1; Table 2). While solute yields in the cave drip water are predominantly bedrock-derived, we identified atmospheric deposition supplies a quantifiable source of trace element species from non-sea salt sources including 20–29% of Na and K and 12–61% of metals such as Al, Cr, Mn, Ni, Co, Cu, Zn and Pb. The non-sea salt constituents include those derived from a complex mixture of anthropogenic emissions from industrial, automobile and coal-fired power stations and aeolian soil and smoke particles (Tadros et al., 2018), illustrating the important role of the atmosphere in providing a direct source of elements to the soil profile above Harrie Wood Cave. Between October 2006 and July 2010, the drier years of our study, drip water Na enrichment (Na/Cl > 0.86) was explained by the additional atmospheric

supply of Na from nss sources (Section 4.3). The interpretation of the declining drip water Na and Cl trend is due to either a reduced frequency of aeolian supplied salts to site i.e. a decrease in aerosol flux over time or a diminishing supply from a major dust storm event that occurred prior to the drip water monitoring period e.g. 2002–03 Australian dust storms (Gabric et al., 2010). We argue that alternate explanations such as geogenic sourcing of Na from halite dissolution can be neglected, confirmed by the mass balance calculations (Table 2). Also, the limestone above and within Harrie Wood Cave, is a fossiliferous micritic limestone with brachiopods and breccias of Silurian age. Soluble minerals such as halite or gypsum would have been removed during diagenesis and the limestone at Yarrangobilly has undergone at least one phase of diagenesis (Gillieson, 2009; Frisia et al., 2018). To date, a considerable number of studies have evaluated the bedrock as a source of solutes acquired from congruent or incongruent dissolution of carbonate minerals (Fairchild et al., 2000; Musgrove and Banner, 2004; Tremaine and Froelich, 2013; Hori et al., 2014; Rutlidge et al., 2014). Comparatively, only a limited number of studies have been done to constrain the atmospheric composition as a source of solutes in karst studies (Baker et al., 2000; Dredge et al., 2013; Tadros et al., 2018).

5.2. Processes influencing drip water ion concentrations

Soil processes regulating the input of metals from these endmember sources in the drip water are summarised in Fig. 4 and were evaluated in this investigation by examining the changing chemistry of the drip waters over time (Fig. 3) in relation to the water solubility of elements in the soil (Table 3). Based on the mass balance (Table 2) and soil enrichment factor results (Fig. 2), the soil zone was recognised as an important sink for trace metals, Na and K and a secondary source for Zn.

Cation exchange processes in the soil were identified to moderate the drip water relationship between Na and Ca, Mg and Sr (Fig. 4a). After the transition to the La Niña phase in July 2010 increased weathering was observed to be consistent with the rise in drip water Ca, Mg and Sr concentrations. Rather than increased weathering rates solely explaining the rise in drip water Ca, Mg and Sr concentrations, evidence from this investigation raises an additional process. From drip water Na concentrations (Fig. 3d) and Na/Cl ratios (Fig. 3e), it was deduced the shift from dry to wet conditions facilitated cation exchange processes; the process of cation exchange by negatively charged clay particles taking Na from solution in exchange for Ca, Mg and Sr (Fig. 3d, g, h and i). For cations with the same valence, the size of the hydrated radius determines exchangeability; where smaller ions are held more tightly to the negatively charged clay surface (Essington, 2004). Thus we hypothesis it is most likely that Mg exchanges with Na, given the larger hydrated radii of Mg (0.428 nm) compared to Ca and Sr (0.412 nm). Sodium build up in the soil from nss atmospheric deposition is surmised to be rapidly dissolved in solution at the onset of the wet period. The low Na drip water concentrations after the shift from dry to wet conditions suggested the uptake of Na from solution by cation exchange; because if Na-rich water is simply flushed out from the soil and diluted, a sharp rise followed by a decrease would have been expected in the drip water time series. Cation exchange by clay minerals is a common hydrogeochemical process that influences the bulk solution during the movement of saline water through aquifer systems (Capaccioni et al., 2005; Argamasilla et al., 2017). Furthermore, if no additional process influenced the drip water, the expected ratio of the infiltrating water would have been on average close to 0.86, given the primary influence of a marine source (Table 2). Alternatively, this decrease in drip water Na/Cl ratios could indicate an accumulation of Cl in the soil. Given that the movement of Cl through the epikarst is largely determined by water flux (Tadros et al., 2016), we infer that Cl is transported conservatively through the soil profile; because it does not complex readily or strongly adsorb to soil components due to the negative charge, or is chemically altered by microbial activity in the
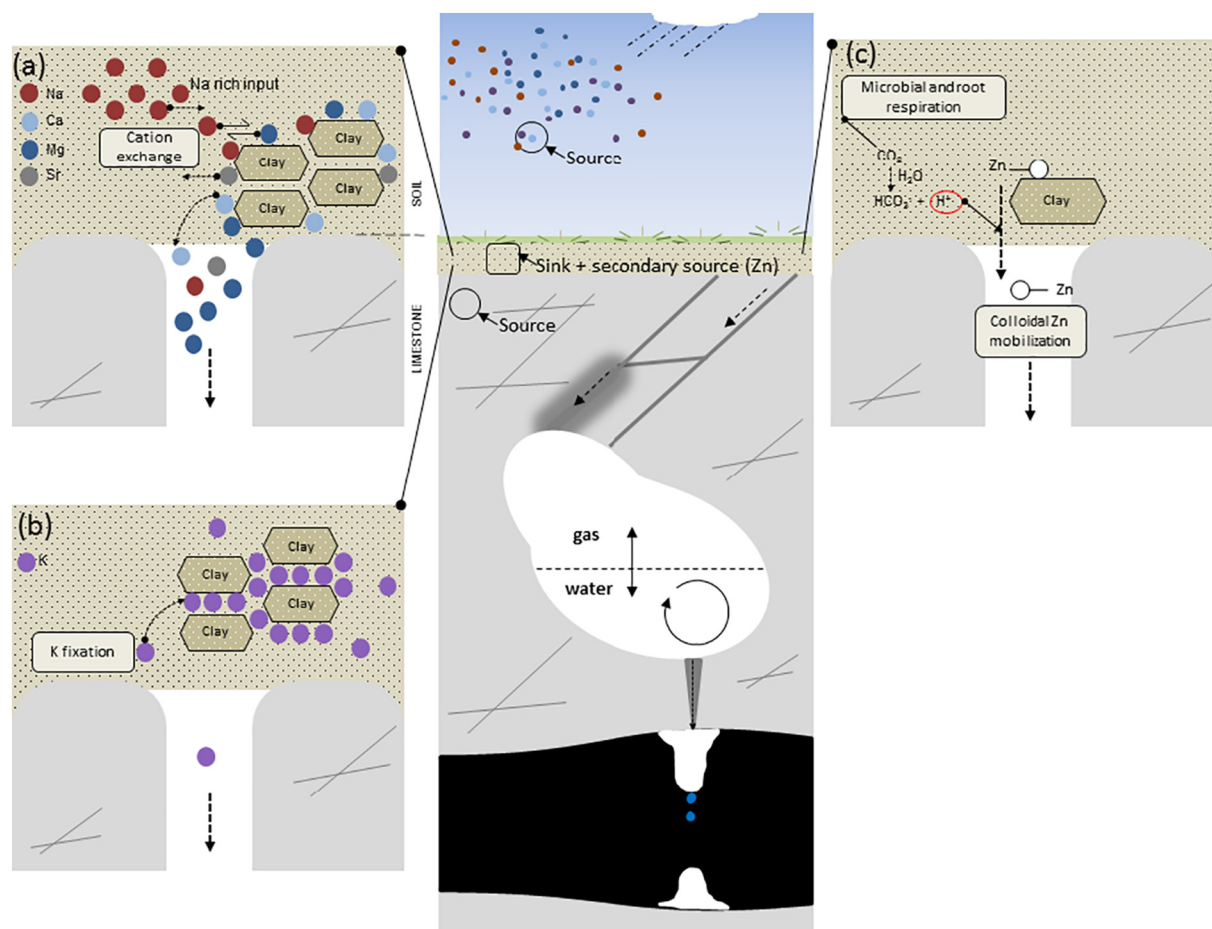
Fig. 4. A schematic representation of several key soil processes that influence drip water hydrochemical variations at Harrie Wood Cave due to a change to the site's cumulative water balance. Ions in cave drip are sourced from aerosols and the bedrock, while the soil zone is a sink for ions and a secondary source for Zn. (a) The shift from dry to wet conditions facilitates cation exchange reactions. Negatively charged clay particles bind Na ions from solution in exchange for cations, in the order Mg > Ca and Sr. (b) Enhanced K-fixation occurs during the sustained dry period, where K balances negatively charged sites in internal clay surfaces and becomes non-exchangeable in solution. K is released into solution as the clay particles are weathered by high rainfall. (c) In soil, Zn is adsorbed on colloidal organic matter. Increased soil CO_2 produced by microbial respiration, dissolves in H_2O releasing bicarbonate (HCO_3^-), and consequently soil pH is lowered via the release of H^+. As the soil becomes acidic, colloidal Zn is mobilised. Finally, mobilised metals which are released into the soil water from processes occurring in (a)–(c) percolate through the soil profile. Adapted from Tadros et al. (2016).

soil (White and Broadley, 2001), hence there is no evidence to support Cl soil enrichment at this study site.

K-fixation by clay minerals in the soil was identified as a fundamental mechanism regulating drip water K during the driest period in the study (Fig. 4b). K is also highly soluble (Table 3), but can easily enter into clay lattices and is selectively fixed in the interlayers of clay minerals. K is trapped between the layers in the clay mineral and is therefore reflected in lower drip-water K concentrations during this period. While during the La Niña event, a greater amount of precipitation led to the slow weathering of the clay structure causing a lagged release of K back into solution. Alternatively, it could be argued that during the dry period soluble K may precipitate as a secondary mineral such as jarsite or alunite minerals (Taylor and Eggleton, 2001). However, we do not favour this explanation, since during the enhanced weathering episode in the dry phase in 2009 and at the onset of the La Niña event in July 2010, concentrations of bedrock derived solutes, including Ca, Mg, Sr in drip-water increased except for K (Section 4.3; Fig. 3j). Furthermore, the formation of a secondary mineral would suggest a source of K, contrary to the mass balance results where a sink was identified (Table 2). Thus the bulk of soluble K in solution is selectively sorbed from solution and is fixed in the interlayers of clay minerals.

Within the soil zone, Zn is adsorbed on colloidal organic matter (Section 4.2) and the large positive Zn residual (Table 2) was attributed to the soil becoming a secondary source of Zn (Section 4.2). Small colloids are known to bind to soil solids (Hartland et al., 2012) and Zn can be bound by colloids in the drip water as described above (Borsato et al., 2007; Fairchild et al., 2010) and the recent results of Frisia et al., 2018. Collecting drip water from the same drip sites examined in this research program (HW1–3) during September 2016, Frisia et al., 2018 determined globular colloidal particles composed of Si, Al and traces of N, Zn, Fe and S precipitate with calcite nanoparticles; inferring the globular colloidal particles were humic-like natural organic matter colloids. Colloidal Zn is proposed to be mobilised under conditions of reduced soil pH (Section 4.2; Fig. 4c). The rise in drip water Zn concentrations in late 2009 supports our proposition of Zn colloidal mobilisation from soils when pH is lowered due to soil respiration and small colloids have been demonstrated to be mobilised by a change in soil pH caused by biogenic CO_2 production (Cruz Jr et al., 2005). The concentration of Zn in the drip water increased after the end of the 2010–12 La Niña in April 2012 (Fig. 3k), simultaneously as the cumulative water balance was beginning to decline. We can infer that this may also be attributed to reduced soil pH from the decomposition of organic matter through respiration with the subsequent release and leaching of Zn. This is plausible; provided there has been organic matter accumulation in the soil in the preceding wet period, which binds more Zn, and the decline in cumulative water balance and progressive soil drying in

2012 provides more oxygen within the soil zone thereby accelerating organic matter degradation; however a more comprehensive examination of Zn mobilisation is warranted.

Previous investigations have shown that the bulk of the soils in the montane region of the Australian Alps are composed of weathered rock (Johnston, 2001) and are known to be influenced by aeolian dust deposits which have high clay content and organic matter (Costin et al., 1952; Costin, 1954; Costin, 1955; Butler, 1956; Chen et al., 2002; Tadros et al., 2018). During the transmission of water from the surface to the stalactite tip, we identify processes within the soil zone involving these clay minerals and colloids, leading to variations in trace and major element concentrations of cave drip water. Understanding how drip water solute load varies as water flows through the clay-rich soil profile in response to changing rainfall and aerosol input has provided important information for identifying the range of trace element proxies which can be used as a palaeo-environmental tool which we discuss in Section 5.3. These findings from Harrie Wood Cave have wider relevance to other karst sites overlain by clay-rich soils, for example Crag Cave, southwest Ireland where the karst area is overlain by a glacial till deposit, which is between 1 to >2 m thickness of clay. By examining varying flow routes through the soil zone matrix and fracture network, Tooth and Fairchild, 2003 identified soil and karst aquifer hydrological controls on Ca, Mg and SO_4 drip water concentrations in response to varying rainfall. This enabled them to conclude that a palaeo-hydrological signal in speleothems at Crag Cave may be interpreted through Mg/Ca ratios. As this current research demonstrates, investigating the effect of soil processes to drip water chemistry yield may provide greater detail on other trace element proxies relevant to the study site.

5.3. Implications for speleothem records

This research demonstrates the significance of modern long-term drip water monitoring as a framework for developing a more robust understanding of sources and processes altering the drip water solute composition as water flows from the surface to the stalactite tip. Although the interpretation of speleothem chemistry from the solution composition can only be done semi-quantitatively due to uncertainties in trace element partitioning and controls on ion incorporation into calcite (Fairchild and Baker, 2012; Day and Henderson, 2013), the results from this and previous studies (Tadros et al., 2016; Tadros et al., 2018) will provide a perspective on, and form the foundation to the expected trends of chemical variations in a stalagmite Holocene record.

Drip water chemistry at Harrie Wood Cave is sensitive to large hydroclimate-driven changes; in particular the Millennium drought and the 2010–12 La Niña (Section 4.3) confirming the suitability of speleothem trace elements as a proxy for drier or wetter climatic periods. Previously, Tadros et al. (2016) demonstrated the sensitivity of known palaeo-climate proxies in the drip waters from Harrie Wood Cave. The Mg/Ca and Sr/Ca ratios in drip waters responded to the Millennium drought and the 2010–12 La Niña period, hence inferring that displacements to higher values would differentiate between dry and wet periods, respectively. In this analysis an additional process impacting Mg, Ca and Sr was identified, although not related to PCP. When rainfall containing a high load of dissolved Na, from aeolian salt deposits on the soil surface, percolated through the clay-rich soil, cation exchange processes occurred releasing Mg, and to a lesser extent Ca and Sr. In this 10-year dataset, ion exchange processes potentially control the concentration of these solutes in solution for six months, whereas PCP dominates variability in the ratios throughout the entire dataset. Thus we infer the PCP process would subsequently exert a greater effect on these solutes in our stalagmite record.

In a subsequent study, Tadros et al. (2018) identified an increase in smoke and soil dust aerosol loadings during below average rainfall conditions and the 2015–16 El Niño period. While this research has shown that soluble elements sourced from aerosol atmospheric input are mediated by processes in the soil zone, variations of the elements Na, K

and Zn in cave stalagmites should be investigated further as potential new proxies for the boundary of these drought and flood events. Quantification of trace element concentrations of Mg, Sr, Na and Zn in cave calcite sample are routinely measured by laser-ablation ICP-MS analyses (LA-ICPMS; Borsato et al., 2007; Fairchild and Treble, 2009) and in principle, trace constituents of these elements, may also be detected in cave calcite to 0.01–10 ppm, using a secondary ionisation mass spectrometer (SIMS; Fairchild and Treble, 2009) and Zn by synchrotron x-ray fluorescence (e.g. Frisia et al., 2018). Given the premise that Na and K measurement by LA-ICPMS is limited due to low mass signal intensities, Na and K can be measured at a detection limit of 10 ppm or better by SIMS (Mason, 1987).

Hartland et al. (2012) demonstrated variations in high-flux and low-flux transportation of trace metals by natural organic matter in cave drip waters, postulating a climatic link to rainfall events. Because of the tendency of Zn to be transported as a colloid in solution (Section 4.3), as a generalisation based on the Zn data, it is envisaged that other colloidal-transported trace metals, for example V, Cr, Co, Ni, Cu, Zn and Pb (Section 4.2; Table 3) will likewise be incorporated in speleothem calcite during periods of decreasing infiltration and could serve as an indicator of drier rainfall conditions. Hence enriched [Trace element/Ca]$_{calcite}$ would most likely parallel periods when the site cumulative water balance reverses to a declining trend, and as suggested by Frisia et al., 2018 expect this could give rise to the solid inclusion of organic matter. Fluorescent lamina has been observed to coincide with high concentrations of colloid-associated trace elements in stalagmite records (Roberts et al., 1998; Huang et al., 2001; Fairchild et al., 2001; Borsato et al., 2007). Hence, future research examining fluorescent regions in stalagmite records at Harrie Wood Cave may provide useful insight for the application of Zn and other colloidal-transported trace metals as a proxy for delineating the termination of a period of high water flux.

In cave drip waters, K concentrations displayed the greatest contrast between distinct extreme phases of water flux at the cave site i.e. Millennium drought event and 2010–12 La Niña flooding event (Fig. 3j), demonstrating it may be a potential palaeo-climate proxy. In a resultant stalagmite record from a karst site overlain by clay-rich soil, it is anticipated that multi-year shifts of [K/Ca]$_{calcite}$ to higher values may reflect the onset of wetter surface conditions. Likewise, a clear contrast in the drip water Na concentrations was observed between the extreme phases of ENSO, with a well-defined drop in Na. Due to the smaller ionic radius of Zn (0.71 Å) compared to Ca (0.99 Å) and with a solubility less than calcite (Log $K_{sp} = -9.82$; Crocket and Winchester, 1966), Zn easily substitutes for Ca in the structure of calcite, however alkali metal co-precipitation with calcite varies. Ishikawa and Ichikuni (1984) and Busenberg and Plummer (1985) proposed that both Na and K ions occupy interstitial sites in the crystal structure of calcite. In an experiment investigating the co-precipitation of alkali metal ions (Li, Na, K and Rb) with calcium carbonate, Okumura and Kitano (1986) confirmed this. In the presence of high Na concentrations in the drip water solution, Pingitore Jr and Eastman (1986) identified that Na may be preferentially incorporated over Sr into non-lattice sites in calcite. Presumably, a greater abundance of Na and K at growth defect sites in calcite from Harrie Wood Cave may imply periods of drought, however this hypothesis must be supported by SIMS and LA-ICPMS analyses (Frisia et al., 2018). Thus, due to the difficulty to predict the incorporation of Na and K from drip water into speleothems, prior to establishing these elements as proxies in speleothem calcite, our results highlight the need to further examine trace element distribution in the calcite structure to aid interpreting calcite geochemistry.

Tadros et al., 2016 demonstrated that the isolated use of oxygen-isotope proxies is limited as no distinct drip water seasonal isotopic response was observed. In this region the modern $\delta^{18}O$ signal in meteoric precipitation is ambiguous (Callow et al., 2014), moreover post infiltration processes have been demonstrated to influence the drip water $\delta^{18}O$ composition (Markowska et al., 2015). However, using a diverse suite of trace elements may be the most promising approach for this site.

6. Conclusions

We demonstrate the usefulness of combining field sampling of end-member data sets with long-term cave drip water monitoring to extensively evaluate the processes controlling changes in the chemical signatures of drip waters under a changing climate. Despite the broad geochemical differences between endmembers, the supply of ions to the drip waters was differentiated using a mass balance approach. Mineral weathering of the local bedrock is the dominant source of Mg, Sr, K and trace elements; however the importance of aerosols in supplying Na, Cl, K and Zn to the bulk soil was recognised.

Following the mass balance approach of Treble et al. (2016), quantitative insight into the sources of dissolved solutes in the drip water was obtained. Here, the approach of Treble et al. (2016) has been extended to quantify the non-sea salt aerosol contribution in the drip water, and by also including transition metals in this investigation. We revealed that the concentration of trace and major elements in drip waters not only depends on sources but highlights the central role of soil zone processes in influencing the drip water composition during the movement of rainfall from the surface to the stalactite tip. Furthermore, this research also took into account soil enrichment factors, relative to local bedrock, which supported the mass balance calculations and confirmed that the soil is a significant sink for the bedrock derived transitional metals. We concluded that the clay-rich soil zone is a significant factor influencing the retention and transfer of metals from soil solution to cave drip waters. These conclusions were hinged on examining changes in a range of major and trace drip water solutes over the longer term and understanding the drip water response during contrasting periods of rainfall conditions. During drought, Na inputs enriching the soil from sources other than marine aerosols may become more important e.g. windblown soil and smoke. At the onset of wetter conditions, the Na-rich input signal was altered in the soil solution by cation exchange. Another prominent process during the drought was K-fixation and the subsequent release to solution under sustained wet conditions. Furthermore, the soil was identified as a secondary source for Zn and was released in solution as colloidal particles.

This research greatly adds to our understanding of the geochemical drip water signal from Harrie Wood Cave, south-eastern Australia and underlie the value of a well-characterised karst system. As such investigations of the sources and processes regulating the mobility of solutes in a modern karst environment allow reliable interpretation of speleothem trace elemental cycles. Tadros et al. (2016) demonstrated that Ca, Mg and Sr can be used as palaeo-environmental proxies for contrasting rainfall conditions; as reduced rainfall invoked prior calcite precipitation (PCP) which lead to an increase in drip water (and hence stalagmite) Mg/Ca and Sr/Ca ratios. Here we show an additional modulation of these solutes from cation exchange, but conclude that the PCP signal will likely dominate in the stalagmite trace element record. We expect that drought periods in the stalagmite-based archive could be detected by using Mg and Sr, however a key insight which arose is that drip water elemental variations in Na, K and Zn show particular promise as useful palaeo-climate proxies, however further research into colloidally-transported trace metals and Na and K partitioning between fluid and speleothems would be beneficial.

Acknowledgements

Appendix A. Supplementary data

Supplementary data to this article can be found online at https://doi.org/10.1016/j.scitotenv.2018.10.035.

References

Adriano, D., 2001. Trace Elements in Terrestrial Environments: Biogeochemistry, Bioavailability and Risks of Metals. Springer, New York (867 pp.).

Aplin, K., Ford, F., Hiscock, P., 2010. Early Holocene human occupation and environment of the southeast Australian Alps: new evidence for the Yarrangobilly Plateau, New South Wales. In: Haberle, Simon, Stevenson, Janelle, Prebble, Matthew (Eds.), Altered Ecologies: Fire, Climate and Human Influence on Terrestrial Landscapes, pp. 187–212.

Argamasilla, M., Barberá, J.A., Andreo, B., 2017. Factors controlling groundwater salinization and hydrogeochemical processes in coastal aquifers from southern Spain. Sci. Total Environ. 580, 50–68. https://doi.org/10.1016/j.scitotenv.2016.11.173.

Au, C.O., 2017. http://apo.org.au/system/files/73419/apo-nid73419-7336.pdf, Accessed date: 30 April 2018.

Baker, A., Genty, D., Fairchild, I.J., 2000. Hydrological characterisation of stalagmite drip waters at grotte de Villars, Dordogne, by the analysis of inorganic species and luminescent organic matter. Hydrol. Earth Syst. Sci. 4 (3), 439–450. https://doi.org/10.5194/hess-4-439-2000.

Baldini, J.U., McDermott, F., Baldini, L.M., Ottley, C.J., Linge, K.L., Clipson, N., Jarvis, K.E., 2012. Identifying short-term and seasonal trends in cave drip water trace element concentrations based on a daily-scale automatically collected drip water dataset. Chem. Geol. 330, 1–16.

BoM, 2017. http://www.bom.gov.au/climate/enso/, Accessed date: 3 August 2017.

Borsato, A., Frisia, S., Fairchild, I.J., Somogyi, A., Susini, J., 2007. Trace element distribution in annual stalagmite laminae mapped by micrometer-resolution X-ray fluorescence: implications for incorporation of environmentally significant species. Geochim. Cosmochim. Acta 71, 1494–1512. https://doi.org/10.1016/j.gca.2006.12.016.

Bowen, H.J.M., 1979. Environmental Chemistry of the Elements. Academic Press (333 pp).

Busenberg, E., Plummer, L.N., 1985. Kinetic and thermodynamic factors controlling the distribution of SO_3^{2-} and Na^+ in calcites and selected aragonites. Geochim. Cosmochim. Acta 49 (3), 713–725. https://doi.org/10.1016/0016-7037(85)90166-8.

Butler, B.E., 1956. Parna: an aeolian clay. Aust. J. Sci. 18, 145–151.

Callow, N., McGowan, H., Warren, L., Speirs, J., 2014. Drivers of precipitation stable isotope variability in an alpine setting, Snowy Mountains, Australia. J. Geophys. Res. Atmos. 119 (6), 3016–3031. https://doi.org/10.1002/2013JD020710.

Capaccioni, B., Didero, M., Paletta, C., Didero, L., 2005. Saline intrusion and refreshening in a multilayer coastal aquifer in the Catania Plain (Sicily, Southern Italy): dynamics of degradation processes according to the hydrochemical characteristics of groundwaters. J. Hydrol. 307 (1–4), 1–16. https://doi.org/10.1016/j.jhydrol.2004.08.037.

Chen, X.Y., Spooner, N.A., Olley, J.M., Questiaux, D.G., 2002. Addition of aeolian dusts to soils in southeastern Australia: red silty clay trapped in dunes bordering Murrumbidgee River in the Wagga Wagga region. Catena 47, 1–27. https://doi.org/10.1016/S0341-8162(01)00176-X.

Chester, R., 2009. Marine Geochemistry. John Wiley & Sons (520 pp).

Chubb, T.H., Siems, S.T., Manton, M.J., 2011. On the decline of wintertime precipitation in the snowy mountains of Southeastern Australia. J. Hydrometeorol. 12 (6), 1483–1497. https://doi.org/10.1175/JHM-D-10-05021.1.

Coleborn, K., Baker, A., Treble, P.C., Andersen, M.S., Baker, A., Tadros, C.V., Tozer, M., Fairchild, I.J., Spate, A., Meehan, S., 2018. The impact of fire on the geochemistry of speleothem-forming drip water in a sub-alpine cave. Sci. Total Environ. 642, 408–420. https://doi.org/10.1016/j.scitotenv.2018.05.310.

Costin, A.B., 1954. A Study of the Ecosystems of the Monaro Region of New South Wales. Government Printer, Sydney.

Costin, A.B., 1955. Alpine soils in Australia with reference to conditions in Europe and New Zealand. J. Soil Sci. 6, 35–50. https://doi.org/10.1111/j.1365-2389.1955.tb00828.x.

Costin, A.B., Hallsworth, E.G., Woof, M., 1952. Studies of pedogenesis in New South Wales. III. The alpine humus soils. J. Soil Sci. 3, 190–218. https://doi.org/10.1111/j.1365-2389.1952.tb00643.x.

Crocket, J.H., Winchester, J.W., 1966. Coprecipitation of zinc with calcium carbonate. Geochim. Cosmochim. Acta 30 (10), 1093–1109. https://doi.org/10.1016/0016-7037(66)90119-0.

Cruz Jr., F.W., Karmann, I., Magdaleno, G.B., Coichev, N., Viana Jr., O., 2005. Influence of hydrological and climatic parameters on spatial-temporal variability of fluorescence intensity and DOC of karst percolation waters in the Santana Cave System, Southeastern Brazil. J. Hydrol. 302 (1–4), 1–12. https://doi.org/10.1016/j.jhydrol.2004.06.012.

Dai, A., Fung, I.Y., Del Genio, A.D., 1997. Surface observed global land precipitation variations during 1900–1988. J. Clim. 10, 2943–2962. https://doi.org/10.1175/1520-0442(1997)010<2943:SOGLPV>2.0.CO;2.

Day, C.C., Henderson, G.M., 2013. Controls on trace-element partitioning in cave-analogue calcite. Geochim. Cosmochim. Acta 120, 612–627. https://doi.org/10.1016/j.gca.2013.05.044.

Dredge, J., Fairchild, I.J., Harrison, R.M., Fernandez-Cortes, A., Sanchez-Moral, S., Jurado, V., Gunn, J., Smith, A., Spötl, C., Mattey, D., Wynn, P.M., Grassineau, N., 2013. Cave aerosols: distribution and contribution to speleothem geochemistry. Quat. Sci. Rev. 63, 23–41.

Drever, J.I., 1997. Catchment Mass Balance. Geochemical Processes, Weathering and Groundwater Recharge in Catchments. 241–261.

Essington, M.E., 2004. Soil and Water Chemistry: An Integrative Approach. CRC press.

Fairchild, I.J., Baker, A., 2012. Speleothem Science: From Process to Past Environments. John Wiley & Sons (416 pp).

Fairchild, I.J., Treble, P.C., 2009. Trace elements in speleothems as recorders of environmental change. Quat. Sci. Rev. 28, 449–468.

Fairchild, I.J., Borsato, A., Tooth, A.F., Frisia, S., Hawkesworth, C.J., Huang, Y., McDermott, F., Spiro, B., 2000. Controls on trace element (Sr–Mg) compositions of carbonate cave waters: implications for speleothem climatic records. Chem. Geol. 166 (3–4), 255–269. https://doi.org/10.1016/S0009-2541(99)00216-8.

Fairchild, I.J., Baker, A., Borsato, A., Frisia, S., Hinton, R.W., McDermott, F., Tooth, A.F., 2001. Annual to sub-annual resolution of multiple trace-element trends in speleothems. J. Geol. Soc. 158 (5), 831–841. https://doi.org/10.1144/jgs.158.5.831.

Fairchild, I.J., Spötl, C., Frisia, S., Borsato, A., Susini, J., Wynn, P.M., Cauzid, J., 2010. Petrology and geochemistry of annually laminated stalagmites from an Alpine cave (Obir, Austria): seasonal cave physiology. Geol. Soc. Lond., Spec. Publ. 336 (1), 295–321. https://doi.org/10.1144/SP336.16.

Frisia, S., Borsato, A., Hellstrom, J., 2018. High spatial resolution investigation of nucleation, growth and early diagenesis in speleothems as exemplar for sedimentary carbonates. Earth Sci. Rev. 178, 68–91. https://doi.org/10.1016/j.earscirev.2018.01.014.

Gabric, A.J., Cropp, R.A., McTainsh, G.H., Johnston, B.M., Butler, H., Tilbrook, B., Keywood, M., 2010. Australian dust storms in 2002–2003 and their impact on Southern Ocean biogeochemistry. Glob. Biogeochem. Cycles 24 (2). https://doi.org/10.1029/2009GB003541.

Gillieson, D., 2009. Caves: Processes, Development and Management. John Wiley & Sons (336 pp).

Greene, R.S.B., Cattle, S.R., McPherson, A.A., 2009. Role of eolian dust deposits in landscape development and soil degradation in southeastern Australia. Aust. J. Earth Sci. 56 (S1), S55–S65. https://doi.org/10.1080/08120090902871101.

Hartland, A., Fairchild, I.J., Lead, J.R., Borsato, A., Baker, A., Frisia, S., Baalousha, M., 2012. From soil to cave: transport of trace metals by natural organic matter in karst dripwaters. Chem. Geol. 304–305, 68–82.

Hooda, P., 2010. Trace Elements in Soils. John Wiley & Sons (616 pp.).

Hori, M., Ishikawa, T., Nagaishi, K., You, C.F., Huang, K.F., Shen, C.C., Kano, A., 2014. Rare earth elements in a stalagmite from southwestern Japan: a potential proxy for chemical weathering. Geochem. J. 48 (1), 73–84. https://doi.org/10.2343/geochemj.2.0287.

Huang, Y., Fairchild, I.J., 2001. Partitioning of Sr2+ and Mg2+ into calcite under karst-analogue experimental conditions. Geochim. Cosmochim. Acta 65 (1), 47–62.

Huang, Y., Fairchild, I.J., Borsato, A., Frisia, S., Cassidy, N.J., McDermott, F., Hawkesworth, C.J., 2001. Seasonal variations in Sr, Mg and P in modern speleothems (Grotta di Ernesto, Italy). Chem. Geol. 175 (3–4), 429–448. https://doi.org/10.1016/S0009-2541(00)00337-5.

Ishikawa, M., Ichikuni, M., 1984. Uptake of sodium and potassium by calcite. Chem. Geol. 42 (1–4), 137–146. https://doi.org/10.1016/0009-2541(84)90010-X.

Johnson, K.R., Hu, C., Belshaw, N.S., Henderson, G.M., 2006. Seasonal trace-element and stable-isotope variations in a Chinese speleothem: the potential for high-resolution paleomonsoon reconstruction. Earth Planet. Sci. Lett. 244 (1–2), 394–407. https://doi.org/10.1016/j.epsl.2006.01.064.

Johnston, S.W., 2001. The influence of aeolian dust deposits on alpine soils in south-eastern Australia. Soil Res. 39 (1), 81–88. https://doi.org/10.1071/SR99121.

Kabata-Pendias, A., 2010. Trace Elements in Soils and Plants. CRC press (548 pp.).

Lucas, C., Hennessy, K., Mills, G., Bathols, J., 2007. Bushfire weather in southeast Australia: recent trends and projected climate change impacts. URL. http://www.cmar.csiro.au/e-print/open/2007/hennesseykj_c.pdf, Accessed date: 1 September 2017.

Ma, L.Q., Rao, G.N., 1997. Chemical fractionation of cadmium, copper, nickel, and zinc in contaminated soils. J. Environ. Qual. 26 (1), 259–264. https://doi.org/10.2134/jeq1997.00472425002600010036x.

Markowska, M., Baker, A., Treble, P.C., Andersen, M.S., Hankin, S., Jex, C.N., Tadros, C.V., Roach, R., 2015. Unsaturated zone hydrology and cave drip discharge water response: implications for speleothem paleoclimate record variability. J. Hydrol. 529, 662–675. https://doi.org/10.1016/j.jhydrol.2014.12.044.

Mason, R.A., 1987. Ion microprobe analysis of trace elements in calcite with an application to the cathodoluminescence zonation of limestone cements from the Lower Carboniferous of South Wales, UK. Chem. Geol. 64 (3–4), 209–224. https://doi.org/10.1016/0009-2541(87)90003-9.

McDonald, J., Drysdale, R., Hill, D., 2004. The 2002–2003 El Niño recorded in Australian cave drip waters: implications for reconstructing rainfall histories using stalagmites. Geophys. Res. Lett. 31.

Musgrove, M., Banner, J.L., 2004. Controls on the spatial and temporal variability of vadose dripwater geochemistry: Edwards aquifer, central Texas. Geochim. Cosmochim. Acta 68 (5), 1007–1020. https://doi.org/10.1016/j.gca.2003.08.014.

Nicholls, N., 2003. Continued anomalous warming in Australia. Geophys. Res. Lett. 30 (7). https://doi.org/10.1029/2003GL017037.

Okumura, M., Kitano, Y., 1986. Coprecipitation of alkali metal ions with calcium carbonate. Geochim. Cosmochim. Acta 50, 49–58. https://doi.org/10.1016/0016-7037(86)90047-5.

Pickering, C.M., Growcock, A.J., 2009. Impacts of experimental trampling on tall alpine herbfields and subalpine grasslands in the Australian Alps. J. Environ. Manag. 91 (2), 532–540.

Pingitore Jr., N.E., Eastman, M.P., 1986. The coprecipitation of Sr2+ with calcite at 25 C and 1 atm. Geochim. Cosmochim. Acta 50 (10), 2195–2203.

Pook, M.J., Risbey, J.S., McIntosh, P.C., 2014. A comparative synoptic climatology of cool-season rainfall in major grain-growing regions of southern Australia. Theor. Appl. Climatol. 117 (3–4), 521–533.

Rayment, G.E., Higginson, F.R., 1992. Australian Laboratory Handbook of Soil and Water Chemical Methods. Inkata Press Pty Ltd (330 pp).

Risbey, J.S., Pook, M.J., McIntosh, P.C., Wheeler, M.C., Hendon, H.H., 2009. On the remote drivers of rainfall variability in Australia. Mon. Weather Rev. 137 (10), 3233–3253. https://doi.org/10.1175/2009MWR2861.1.

Roberts, M.S., Smart, P.L., Baker, A., 1998. Annual trace element variations in a Holocene speleothem. Earth Planet. Sci. Lett. 154 (1–4), 237–246. https://doi.org/10.1016/S0012-821X(97)00116-7.

Rutlidge, H., Baker, A., Marjo, C.E., Andersen, M.S., Graham, P.W., Cuthbert, M.O., Rau, G.C., Roshan, H., Markowska, M., Mariethoz, G., Jex, C.N., 2014. Dripwater organic matter and trace element geochemistry in a semi-arid karst environment: implications for speleothem paleoclimatology. Geochim. Cosmochim. Acta 135, 217–230. https://doi.org/10.1016/j.gca.2014.03.036.

Sarnat, J.A., Long, C.M., Koutrakis, P., Coull, B.A., Schwartz, J., Suh, H.H., 2002. Using sulfur as a tracer of outdoor fine particulate matter. Environ. Sci. Technol. 36 (24), 5305–5314.

Shao, Y., Klose, M., Wyrwoll, K.H., 2013. Recent global dust trend and connections to climate forcing. J. Geophys. Res. Atmos. 118 (19). https://doi.org/10.1002/jgrd.50836.

Siklosy, Z., Demeny, A., Vennemann, T.W., Pilet, S., Kramers, J., Leél-Őssy, S., Bondár, M., Shen, C.C., Hegner, E., 2009. Bronze Age volcanic event recorded in stalagmites by combined isotope and trace element studies. Rapid Commun. Mass Spectrom. 23 (6), 801–808. https://doi.org/10.1002/rcm.3943.

Speer, M.S., 2013. Dust storm frequency and impact over Eastern Australia determined by state of Pacific climate system. Weather Clim. Extremes 2, 16–21. https://doi.org/10.1016/j.wace.2013.10.004.

Sturman, A.P., Tapper, N.J., 1996. The Weather and Climate of Australia and New Zealand. Oxford University Press (476 pp).

Sundqvist, H.S., Holmgren, K., Fohlmeister, J., Zhang, Q., Matthews, M.B., Spötl, C., Körnich, H., 2013. Evidence of a large cooling between 1690 and 1740 AD in southern Africa. Sci. Rep. 3, 1767. https://doi.org/10.1038/srep01767.

Tadros, C.V., Treble, P.C., Baker, A., Fairchild, I., Hankin, S., Roach, R., Markowska, M., McDonald, J., 2016. ENSO–cave drip water hydrochemical relationship: a 7-year dataset from south-eastern Australia. Hydrol. Earth Syst. Sci. 20, 4625–4640. https://doi.org/10.5194/hess-20-4625-2016.

Tadros, C.V., Crawford, J., Treble, P.C., Baker, A., Cohen, D.D., Atanacio, A.J., Hankin, S., Roach, R., 2018. Chemical characterisation and source identification of atmospheric aerosols in the Snowy Mountains, south-eastern Australia. Sci. Total Environ. 630, 432–443. https://doi.org/10.1016/j.scitotenv.2018.02.231.

Taylor, G., Eggleton, R.A., 2001. Regolith Geology and Geomorphology. John Wiley & Sons (375 pp).

Taylor, S.R., McLennan, S.M., 1995. The geochemical evolution of the continental crust. Rev. Geophys. 33 (2), 241–265. https://doi.org/10.1029/95RG00262.

Tessier, A., Campbell, P.G., Bisson, M., 1979. Sequential extraction procedure for the speciation of particulate trace metals. Anal. Chem. 51 (7), 844–851.

Theobald, A., McGowan, H., Speirs, J., 2016. Trends in synoptic circulation and precipitation in the Snowy Mountains region, Australia, in the period 1958–2012. Atmos. Res. 169, 434–448. https://doi.org/10.1016/j.atmosres.2015.05.007.

Tomasi, C., Fuzzi, S., Kokhanovsky, A. (Eds.), 2017. Atmospheric Aerosols: Life Cycles and Effects on Air Quality and Climate. Vol. 1. John Wiley & Sons (704 pp).

Tooth, A.F., Fairchild, I.J., 2003. Soil and karst aquifer hydrological controls on the geochemical evolution of speleothem-forming drip waters, Crag Cave, southwest Ireland. J. Hydrol. 273, 51–68.

Treble, P.C., Fairchild, I.J., Baker, A., Meredith, K.M., Andersen, M.S., Salmon, S.U., Bradley, C., Wynn, P.M., Hankin, S., Wood, A., McGuire, E., 2016. Roles of bioproductivity, transpiration and fire in a nine-year record of cave dripwater chemistry from southwest Australia. Geochim. Cosmochim. Acta https://doi.org/10.1016/j.gca.2016.04.017.

Tremaine, D.M., Froelich, P.N., 2013. Speleothem trace element signatures: a hydrologic geochemical study of modern cave dripwaters and farmed calcite. Geochim. Cosmochim. Acta 121, 522–545. https://doi.org/10.1016/j.gca.2013.07.026.

Turekian, K.K., 1968. Oceans. Foundations of Earth Science Series. Prentice-Hall (120 pp).

White, P.J., Broadley, M.R., 2001. Chloride in soils and its uptake and movement within the plant: a review. Ann. Bot. 88 (6), 967–988. https://doi.org/10.1006/anbo.2001.1540.

Wotawa, G., Trainer, M., 2000. The influence of Canadian forest fires on pollutant concentrations in the United States. Science 288 (5464), 324–328. https://doi.org/10.1126/science.288.5464.324.